Tetrahedron Vol. 48, No. 20, pp. 4193-4208, 1992
Printed in Great Britain

0040-4020/92 $5.00+.00

A NEW SYNTHESIS OF 6-OXOPYRIMIDINIUM-4-OLATES. THEORETICAL STUDY OF THE REGIOSELECTIVE CYCLOADDITION OF ARYLISOCYANATES WITH A 1,3-THIAZOLIUM-4-OLATE SYSTEM

Martín Avalos[a], Reyes Babiano[a], María J. Diánez[b], Joaquín Espinosa[c], María D. Estrada[b], José L. Jiménez[a], Amparo López-Castro[b], María M. Méndez[a], Juan C. Palacios[a]

Departamento de Química Orgánica[a] and Departamento de Química Física[c], Universidad de Extremadura, 06071 Badajoz, Spain, and Instituto de Ciencias de Materiales de Sevilla[b], C.S.I.C., Universidad de Sevilla, 41071, Sevilla, Spain

(*Received in UK 24 March* 1992)

Abstract. A new and regioselective synthesis of 6-oxopyrimidinium-4-olate systems (**13-21**) is described, involving the 1,3-dipolar cycloaddition of the 1,3-thiazolium-4-olate **12** with arylisocyanates. MNDO and AM1 calculations rationalise the reactivity and regioselectivity experimentally observed.

Introduction

Considerable effort has been devoted to the 1,3-dipolar cycloaddition of mesoionic ring systems (**1**) with heterocumulenes[1,2]. Depending on the fragment extruded from the initial 1:1 cycloadduct (**2**), the reaction provides new mesoionic heterocycles (**3**) or six-membered heteroaromatic betaines (**4**) (Scheme 1).

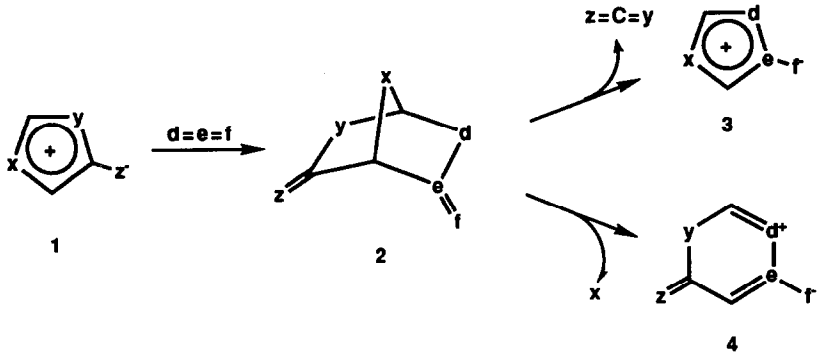

Scheme 1

Potts *et al.*[3-5] have described the formation of stable 1:1 cycloadducts (**6**) when isocyanates and isothiocyanates were used as heterocumulenes. However, later, Hamaguchi and Nagai[6] have demonstrated the

mesoionic nature (**8**) of these compounds. These authors have proposed a concerted cycloaddition pathway followed by the ring opening of **6** to give **8** *via* the dipolar intermediate **7** (Scheme 2).

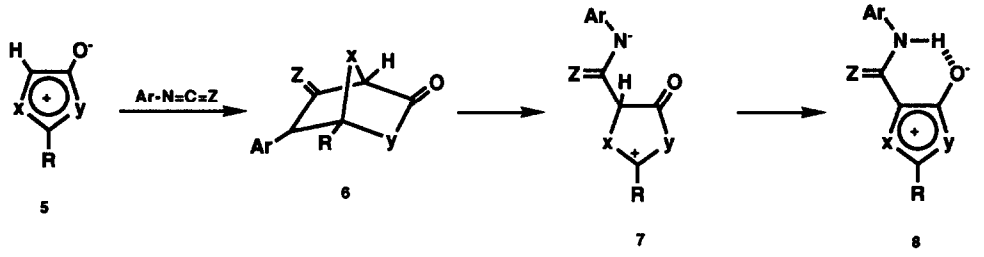

Scheme 2

On the other hand, Potts *et al.*[7] have described the conversion of the 1,3-selenazolium-4-olate system (**9**) into a six-membered heteroaromatic betaine **11** when the mesoionic heterocycle was refluxed with phenylisothiocyanate (Scheme 3).

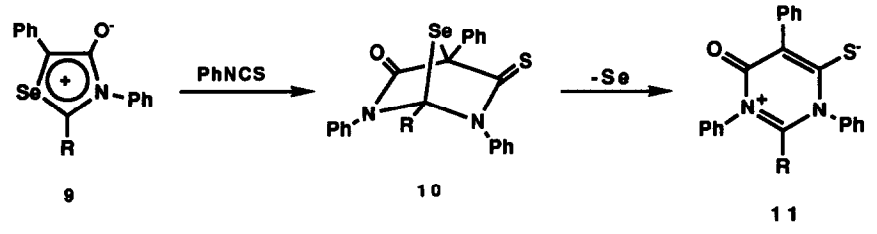

Scheme 3

This synthetic sequence represents the first conversion of a five-membered mesoionic ring into a six-membered heteroaromatic betaine by reaction with heterocumulenes[8].

Although the ease with which selenium was extruded from **10** was proposed[7] as cause of formation of **11**, the presence of a substituent in C-5 could be also responsible of this behaviour, preventing a similar rearrangement to that showed in the last step of Scheme 2.

In this paper we have studied the reaction of the related per-substituted 1,3-thiazolium-4-olate system (**12**)[9] with arylisocyanates. In all cases a 6-oxopyrimidinium-4-olate system (**13-21**) was formed. This type of heterocycle was only accessible by reaction of an amidine system with dialkyl malonates or their synthetic equivalents[10,11]. Our reaction opens a new route to these betaines. Moreover, with the aim of giving an interpretation of the regioselectivity of this reaction, we have performed semiempirical AM1 and MNDO molecular orbital studies.

Results and Discussion

The starting 1,3-thiazolium-4-olate **12** was prepared from 2-amino-2-deoxy-α-D-glucopyranose hydrochloride in four steps[9]. Its 1,3-dipolar cycloaddition with arylisocyanates were carried out in benzene at

reflux for several hours and led in all cases to the cross-conjugated heterocyclic mesomeric betaines **13-21**. The alternative conjugated heterocyclic mesomeric betaines **22** were not detected.

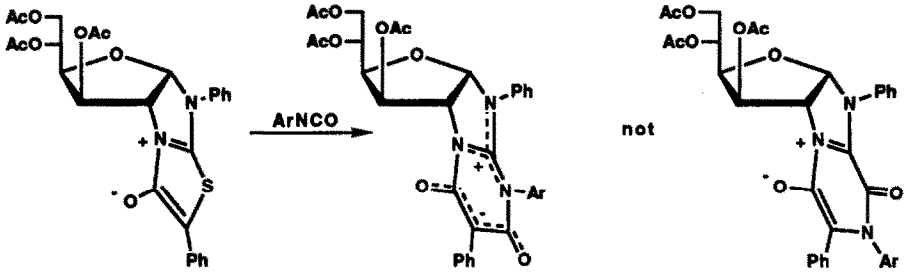

12 **22**

13 Ar = 4-$CH_3OC_6H_4$
14 Ar = 4-ClC_6H_4
15 Ar = 4-$NO_2C_6H_4$
16 Ar = 3-$CH_3OC_6H_4$
17 Ar = 3-ClC_6H_4
18 Ar = 3-$NO_2C_6H_4$
19 Ar = 2-$CH_3OC_6H_4$
20 Ar = 2-ClC_6H_4
21 Ar = 2-$NO_2C_6H_4$

Scheme 4

Crystalline structure of 13.

The structure of **13** was confirmed by X-ray crystallographic analysis. A perspective view of the molecule in the solid state, showing the relative configuration and the atomic numbering scheme, is given in Figure 1.

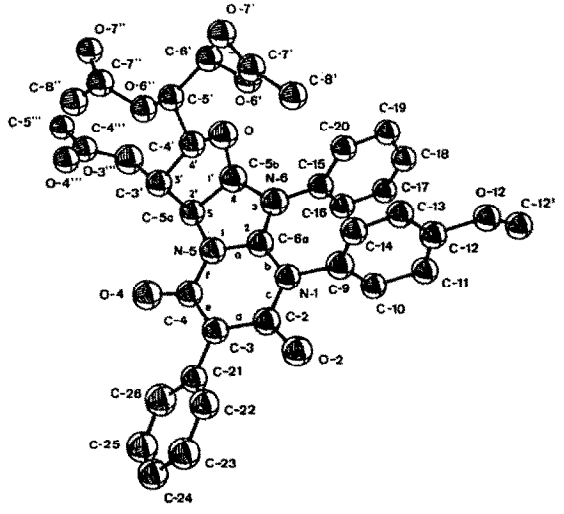

Figure 1

Several bond lengths and bond angles appear in Tables I and II. The mean value C-C in the phenyl groups is 1.34(4) Å. The imidazoline and 4,6-dioxopyrimidine rings are planar, and the maximun deviations from the best planes are 0.02 and 0.06 Å, respectively. The C-15, C-9, and C-21 substituents are at 0.31, -0.13, and 0.05 Å from the respective ring best planes. The three phenyl and three O-acetyl groups are also planar and the maximun deviations are 0.03 and 0.05 Å, respectively. The values of C-O, C-C, and C-N bonds in the 4,6-dioxopyrimidine and imidazoline rings indicate some electronic delocalization, in agreement with other spectroscopic results. In the furanose ring, the C-C distances are in the range 1.50(3)-1.55(3) Å.

Table I. Values of bond lengths (Å) from X-Ray analysis of 13

O-3'''	—	C-3'	1.46 (2)	C-3'	—	C-5a	1.50 (2)
N-5	—	C-4	1.40 (2)	C-3'	—	C-4'	1.54 (2)
N-5	—	C-6a	1.33 (2)	C-21	—	C-3	1.47 (2)
N-5	—	C-5a	1.45 (2)	C-6a	—	N-6	1.36 (2)
O-2	—	C-2	1.24 (2)	C-5a	—	C-5b	1.54 (2)
O-4	—	C-4	1.26 (2)	C-5'	—	C-4'	1.50 (2)
N-1	—	C-2	1.40 (2)	C-4'	—	O	1.38 (2)
N-1	—	C-9	1.47 (2)	O	—	C-5b	1.40 (2)
N-1	—	C-6a	1.34 (2)	N-6	—	C-5b	1.47 (3)
C-2	—	C-3	1.43 (2)	N-6	—	C-15	1.42 (3)
C-4	—	C-3	1.38 (3)				

Table II. Values of bond angles (°) from X-Ray analysis of 13

C-6a	—	N-5	—	C-5a	110.9 (16)	C-2	—	C-3	—	C-4	117.4 (17)
C-4	—	N-5	—	C-5a	125.5 (17)	N-5	—	C-6a	—	N-1	119.8 (18)
C-4	—	N-5	—	C-6a	122.7 (18)	N-1	—	C-6a	—	N-6	128.3 (20)
C-9	—	N-1	—	C-6a	119.2 (16)	N-5	—	C-6a	—	N-6	111.8 (19)
C-2	—	N-1	—	C-6a	120.8 (17)	N-5	—	C-5a	—	C-3'	109.8 (18)
C-2	—	N-1	—	C-9	119.6 (17)	C-3'	—	C-5a	—	C-5b	103.1 (15)
O-2	—	C-2	—	N-1	114.3 (19)	N-5	—	C-5a	—	C-5b	104.1 (17)
N-1	—	C-2	—	C-3	119.6 (18)	C-3'	—	C-4'	—	C-5'	117.6 (17)
O-2	—	C-2	—	C-3	125.9 (19)	C-5'	—	C-4'	—	O	109.1 (16)
N-5	—	C-4	—	O-4	113.3 (19)	C-3'	—	C-4'	—	O	105.0 (15)
O-4	—	C-4	—	C-3	127.4 (19)	C-4'	—	O	—	C-5b	106.1 (15)
N-5	—	C-4	—	C-3	119.1 (18)	C-6a	—	N-6	—	C-15	130.7 (20)
O-3'''	—	C-3'	—	C-4'	107.9 (17)	C-6a	—	N-6	—	C-5b	109.8 (17)
O-3'''	—	C-3'	—	C-5a	107.1 (16)	C-5b	—	N-6	—	C-15	117.8 (19)
C-5a	—	C-3'	—	C-4'	100.7 (16)	O	—	C-5b	—	N-6	110.5 (16)
C-4	—	C-3	—	C-21	123.6 (18)	C-5a	—	C-5b	—	N-6	103.1 (17)
C-2	—	C-3	—	C-21	118.9 (18)	C-5a	—	C-5b	—	O	107.8 (16)

In terms of ring-puckering coordinates[12], the amplitude and phase magnitudes are Q=0.38(2) Å and Ψ=39(3)° for the atomic sequence O-$C_{4'}$-$C_{3'}$-C_{5a}-C_{5b}. The asymmetry parameters[13] are ΔC_s (C-4') = 0.012(11) and ΔC_2 (C-5a) = 0.078(8) and ΔC_2 (C-5b) = 0.063(8), so that the conformation is an envelope with a pseudo-mirror plane through C-4'. The substituents are: $O_{3'''}$ axial and $C_{5'}$ quasi-equatorial. The angles between planes are: pyrimidine-imidazoline, 4°; furanose-imidazoline, 105°; phenyl-imidazoline, 41°; pyrimidine-methoxyphenyl, 76°; and pyrimidine-phenyl, 41°.

Table III. ^{1}H-NMR chemical shifts (ppm) for 12-21[a]

Comp	H-1	H-2	H-3	H-4	H-5	H-6	H-6′	OAc	OMe
12	6.56d	5.67d	6.17d	4.17dd	5.32m	4.49dd	4.09dd	2.17s, 1.98s, 1.89s	
13	5.60d	5.04d	6.18d	4.31dd	5.16m	4.48dd	4.11dd	2.14s, 2.12s, 2.02s	3.56s
14	5.60d	5.02d	6.14d	4.30dd	5.16m	4.46dd	4.11dd	2.14s, 2.11s, 2.01s	
15	5.71d	5.09d	6.17d	4.34dd	5.20m	4.48dd	4.15dd	2.14s, 2.11s, 2.01s	
16	5.69d	5.09d	6.19d	4.37dd	5.17m	4.50dd	4.14dd	2.13s, 2.11s, 2.02s	3.61s
	5.52d	5.00d	6.14d	4.28dd	5.17m	4.48dd	4.12dd		3.39s
17	5.63d	5.06d	6.16d	4.35dd	5.17m	4.51dd	4.15dd	2.16s, 2.13s, 2.09s	
	5.46d	4.93d	6.11d	4.30dd	5.17m	4.45dd	4.10dd	2.01s, 2.00s	
18	5.72d	5.12d	6.20d	4.47dd	5.17m	4.53dd	4.09dd	2.19s, 2.14s, 2.09s	
	5.47d	4.95d	6.13d	4.26dd	5.17m	4.44dd	4.14dd	2.03s, 2.00s	
19	5.61d	5.07d	6.25d	4.38dd	5.21m	4.66dd	4.07dd	2.13s, 2.12s, 2.03s	3.75s
20	5.75d	5.21d	6.20d	4.38dd	5.10m	4.44dd	4.08dd	2.16s, 2.15s, 2.13s	
	5.62d	5.08d	6.24d	4.44dd	5.10m	4.59dd	4.14dd	2.04s	
21	5.55d	5.08d	6.26d	4.61dd	5.15m	4.53dd	4.13dd	2.17s, 2.13s, 2.05s	
	5.75d	5.26d	6.19d	4.42dd	5.21m	4.52dd	4.24dd	2.14s, 2.07s, 2.04s	

[a]In $CDCl_3$

Table IV. ^{1}H-N.m.r. coupling constants (Hz) for 12-21[a]

Comp.	$J_{1,2}$	$J_{2,3}$	$J_{3,4}$	$J_{4,5}$	$J_{5,6}$	$J_{5,6'}$	$J_{6,6'}$
12	6.2	0.0	2.7	9.4	2.3	5.0	12.3
13	6.6	0.0	2.7	9.5	2.2	4.4	12.2
14	6.6	0.0	2.8	9.5	2.4	4.7	12.4
15	6.6	0.0	2.6	9.4	2.1	4.4	12.3
16	6.6	0.0	2.7	9.9	2.8	3.4	12.4
	6.6	0.0	2.8	9.6	1.4	4.8	12.4
17	6.6	0.0	2.7	9.6	2.0	4.1	13.0
	6.2	0.0	2.6	10.1	2.1	4.6	12.6
18	6.6	0.0	2.7	9.4		3.7	12.3
	6.5	0.0	2.5	9.2		3.9	12.4
19	6.5	0.0	2.6	9.7	2.6	4.7	12.0
20	6.4	0.0	2.4	9.5		4.6	12.3
	6.5	0.0	2.3		2.1	4.4	12.3
21	6.4	0.0	2.5	9.7	2.7	3.3	12.3
	6.6	0.0	2.8	9.2	2.9	4.5	12.4

[a]Conditions described in Table III

Table V. ^{13}C-NMR chemical shifts (ppm) for 13-21

										Acetate	
Comp	C-1'	C-2'	C-3'	C-4'	C-5'	C-6'	C-2,4	C-3	C-6a	C=O	CH_3
13	94.55	66.47	72.48	76.36	64.25	62.92	159.68 159.52	89.83	149.15	170.25 169.70 168.41	20.68 20.59
14	94.60	66.45	72.36	76.73	64.22	62.79	159.21 156.92	89.67	148.88	170.22 169.61 162.44	20.62 20.54
15	94.71	66.55	72.36	77.00	64.45	62.78	158.75 156.88	89.72	148.71	170.38 169.65 168.56	20.76 20.69 20.62
16	94.74 94.55	66.42	72.47	76.57	64.18	62.88 62.79	159.39 159.34 159.18	89.83 89.78	148.86 148.79	170.34 170.20 169.67 168.36	20.64 20.57 20.53
17	94.61	66.40	72.35	76.66 76.51	64.25	60.15	159.02 156.82 156.75	89.67 89.56	148.65 148.60	170.28 170.19 169.60 168.67 168.31	20.68 20.51 20.50
18	94.79	66.53	72.50	76.85	64.59	62.64	158.86 156.78	89.84	148.68	170.62 169.73 168.36	20.72 20.70 20.59
	94.64	66.53	72.48	76.85	64.42	62.91	158.73 156.84	89.74	140.70	170.34 169.64 168.36	
19	94.31	66.50	72.70	77.00	64.27	62.88	159.16 156.98	89.77	140.03	170.26 169.70 168.33	20.69 20.58
20	94.47	66.51	72.47	77.00	64.32	62.88	158.40 156.87	89.61	148.38	170.27 169.67 168.57	20.75 20.72 20.65
			72.60	76.90	64.45	62.75	158.53 156.85	89.73	148.72	170.40 169.82 168.25	20.55
21	94.43	66.75	72.65	76.67	64.54	62.40	158.66 156.98	90.04	148.75	170.83 170.01 168.32	20.83 20.69 20.61

Crystal packing is mainly due to van der Waals contacts, and there is also a weak intermolecular H-bond, $C_{5a} \cdots O_2$ (x-1,y,z) = 3.11(3) Å; C_{5a}-H$\cdots O_2$ = 139(1)°.

Spectroscopic data.

The ^{1}H-n.m.r. spectroscopic data for **13-21** are given in Tables III and IV. The most characteristic signals are due to the sugar moiety and are analogous to that of similar furanoid bicyclic sugars[9,14,15]. It is remarkable that the presence of the pyrimidine ring induces important differences in the chemical shifts of the H-1 and H-2 proton signals, respect to that of **12**. Thus, H-1 protons of **13-21** undergo strong upfield shifts (~1.0 p.p.m.) due to the shielding produced by the *N*-phenyl group, that is rotated out of the pyrimidine plane. Likewise, H-2 is shifted upfield in **13-21** (~0.6 p.p.m.), respect to H-2 of **12**. In this case, the high negative charge density of the neighbouring oxygen could be responsible of this effect.

^{13}C-n.m.r. spectroscopic data (Table V) are in accord with assigned structures. Both, ^{1}H- and ^{13}C-n.m.r. spectra of **16-21** showed two set of signals due to the presence of atropisomers arising from the restricted rotation around the N-aryl bond. Dynamic n.m.r. investigation at variable temperature allowed to determine the corresponding free energies of activation ($\Delta G^{\neq}$) at the coalescence temperature, T_c. For the exchange between two equally populated sites, $\Delta G^{\neq}$ was approximately calculated for **16-18** (Table VI) using the equation (1)[16]:

$$\Delta G^{\neq} = R\,T_c \ln [(k_B\,T_c\,2^{1/2}) / (\pi\,h\,\Delta\nu)] \qquad (1)$$

when R, k_B, and h denote the gas, Boltzmann and Planck's constants, respectively, whereas $\Delta\nu$ represents the frequency difference between the exchanging sites.

The atropisomeric ratio remains unchanged when the probe was cooled to room temperature from the coalescence temperature (see Table VI). This results are in accordance with the calculated $\Delta G^{\neq}$ for **16-18** because it is well known that a barrier to rotation of ~96 KJ.mol^{-1} is required for stable rotamers at 20°C.

Table VI

Comp.	T_c[a]	$\Delta\nu$[b]	$\Delta G^{\neq}$[c]	K_{eq}[d]
16	343	16.2	74.2	1.05[e]
17	343	14.5	74.5	1.34
18	353	26.5	75.0	1.45

[a] °K, [b] Hz, [c] KJ.mol^{-1}, [d] Calculated at 25°C from H-1 signal integration, [e] This value is identical to measured from OCH_3 signal integration.

For **19-21**, the initial proportion of both atropisomers was changing with the increasing of temperature to reach a constant relationship (1.7, 1.1, and 1.5, respectively) which remained unchanged after heating at 180°C for 3 h. In these cases, the coalescence temperature was not reached below 200°. These high rotation barriers (>98 KJ.mol^{-1}) would imply the existence of stable rotamers at room temperature. Thus, in the case of **21** the major atropisomer could be isolated from the mixture by fractionated crystallisation.

The mass spectra are in accord with the proposed structures. In all cases typical losses of acetic acid, ketene and sugar fragments are observed[17].

Regioselectivity. Theoretical calculations.

The formation of **13-21** must be occur from the initial 1:1 cycloadduct **23** by elimination of sulphur under the reaction conditions. Although **23** could not be isolated or detected, a structurally related compound, the 1:1 cycloaduct **24**, has been obtained as the major product in the reaction of **12** with diethyl azodicarboxylate[18].

The alternative regioisomeric betaine **22** might be formed through an analogous fragmentation of the corresponding sulfur-containing intermediate **25**.

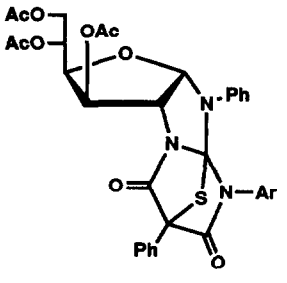

23

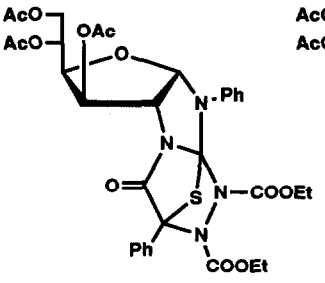

24

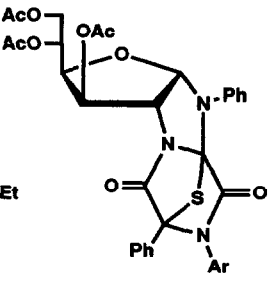

25

Theoretical calculations by several methods have been applied to the study of the reaction of 1,3--thiazolium-4-olate systems with olefinic and acetylenic dipolarophiles[19], but to our knowledge, a theoretical approximation to the reactivity of this mesoionic heterocycle with heterocumulenes have not been previously described. Due to the big size of our molecules we have simplified the calculation taking as model the hypothetical reaction showed in the Scheme 5.

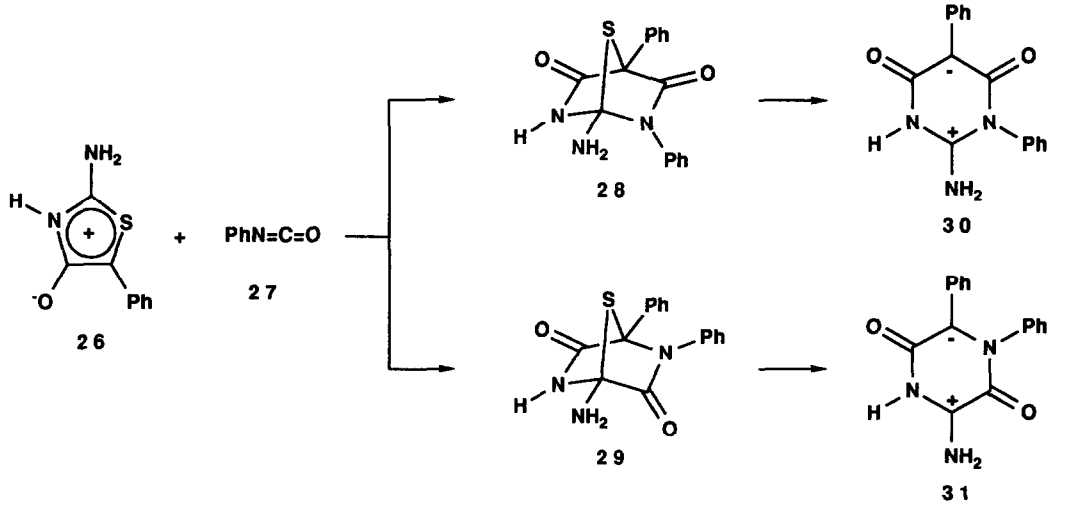

26 + PhN=C=O **27**

28 **29** **30** **31**

Scheme 5

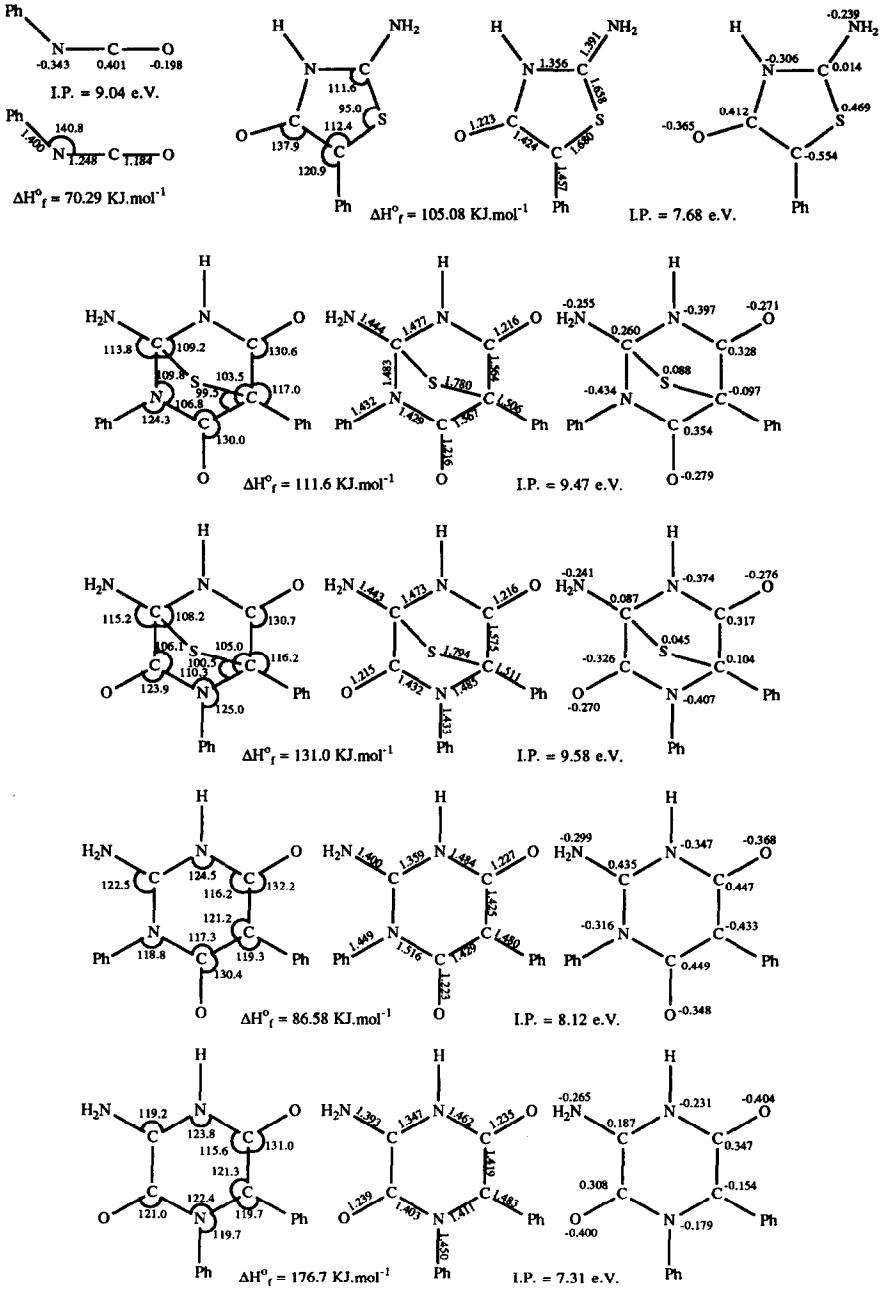

Figure 2. Geometrical parameters, formal charge distributions, heats of formation and ionization potentials for **26-31** calculated from MNDO method

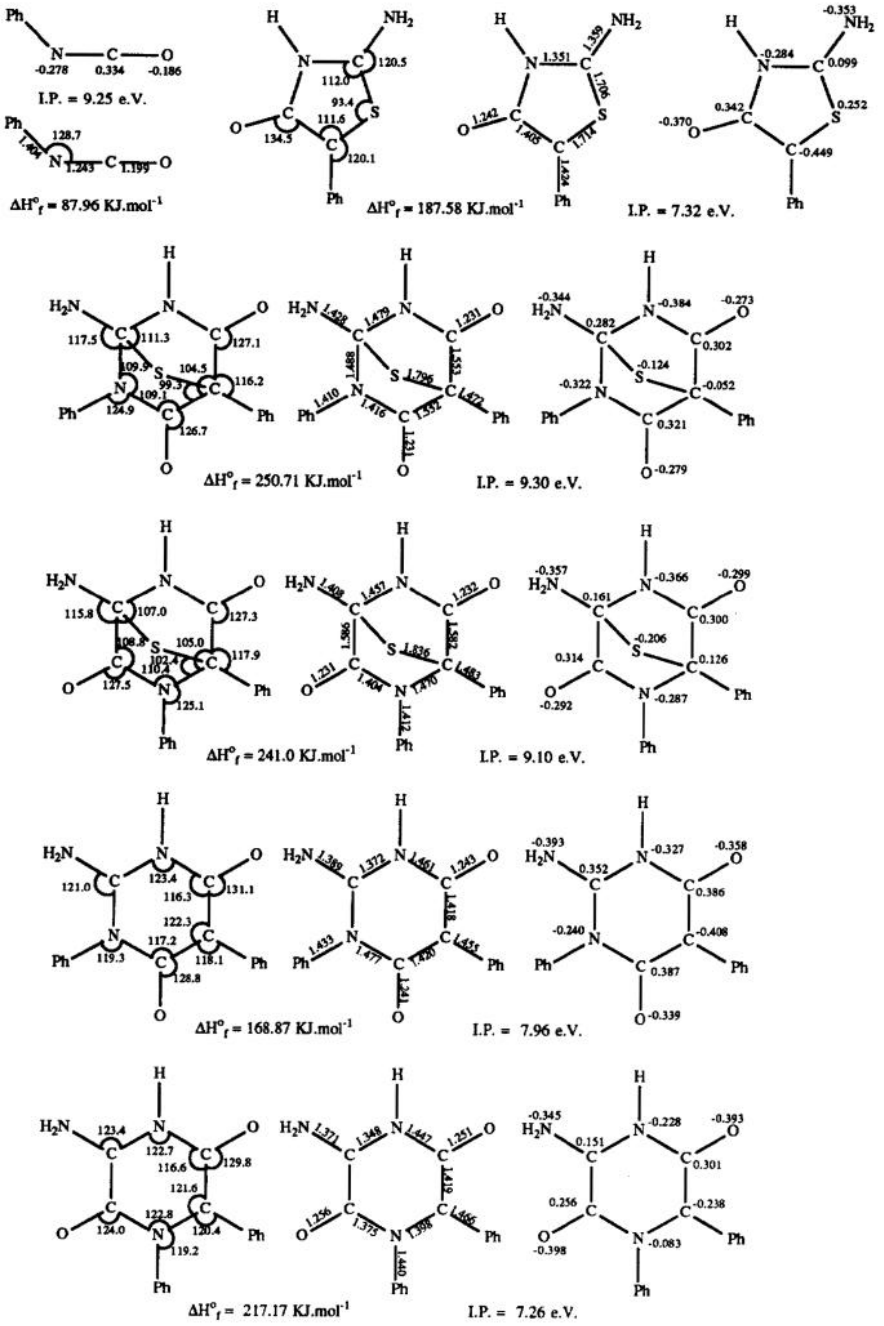

Figure 3. Geometrical parameters, formal charge distributions, heats of formation, and ionization potentials for **26-31** calculated from AM1 method

Figures 2 and 3 contain the more important geometrical parameters (bond lengths and bond angles), formal charge distributions, heats of formation (ΔH°_{f}) and ionization potentials for **26-31** for MNDO[20] and AM1[21], respectively. The dipolar nature of **26**, **30**, and **31** is well reproduced for both, charge distributions (positive partial charges on the heterocycle and negative ones on the exocyclic oxygen atoms), and geometrical data (flattened ring). The presence of sulphur in **28** and **29** leads to the ring bending with C-S-C angles of 81-84° that supposes a lower ring strain.

Phenyl groups are not in the same plane of the betaines (deviations of ~65° for **30** and ~80° for **31** have been found) due to the steric interactions between all substituents. This fact diminishes the electronic delocalization and increases the total energy of system.

A relative comparison of the heats of formation of **26-31** is showed in Table VII for MNDO and AM1 calculations, respectively.

Table VII. Relative stabilities of 28-31 respect to 26 + 27

Comp.	$\Delta(\Delta H_f)^{a,b}$	
	MNDO	AM1
28	-63.77	-24.83
29	-44.37	-34.54
30	-88.79	-106.67
31	+1.33	-58.37

[a] $\Delta(\Delta H_f) = \Delta H_{f\,(comp)} - (\Delta H_{f\,(26)} + \Delta H_{f\,(27)})$ [b] In $KJ.mol^{-1}$

Values from MNDO calculations are indicative of the greater thermodynamic stability of **28** and **30** respect to **29** and **31**. The energy difference between **30** and **31** is 90.5 $KJ.mol^{-1}$, whereas **28** and **29** are only separated by 19.5 $KJ.mol^{-1}$. If the slow step of the reaction involves the formation of the sulphur-containing 1:1 cycloadduct, as it has been postulated for related processes[1,19] the energy difference between **28** and **29** would affect to the stability of the corresponding transition states. Thus, **28** would be thermodynamically and, probably, kinetically favoured over **29**, in accordance with our experimental results.

However, data from the AM1 calculations conclude that, although **30** would be again the more stable betaine, the formation of the intermediate 1:1 cycloadduct **28** is slightly less favoured than that of **29** (9.71 $KJ.mol^{-1}$). This result could be indicative of a thermodynamic control for the overall reaction. However, it is well known that AM1 methods also claim to account possible interactions for hydrogen bonding. Intramolecular hydrogen bond formation requires[22] that the functional groups approach each other at least about 3.4 Å. The N–H----O distance is 2.34 Å (2.56 Å from MNDO) for **31** and 2.55 Å (2.99 Å from MNDO) for **29**. This fact must lead to a stabilization of **29** and **31** respect to **28** and **30**, only ascribable to the used method. On the other hand, the energy difference between **28** and **29** is in the same order that the average error of the method. In addition, the high experimental regioselectivity would be in according with which **28** is both, the kinetically and thermodynamically controlled product.

The second-order PMO theory has been previously applied to the study of the reactivity and regioselectivity observed in similar reactions[19,23]. Under the consideration that Coulombic forces can be neglected, the interaction energy between FMO's of this mesoionic system and those of the arylisocyanate, that lead to **28**, can be calculated from the equation (2)[24] where C_{2HO}, C_{2LU}, C_{5HO}, and C_{5LU} refers to the $2p_z$ atomic orbital's

coeficients on the 2 and 5 carbon atoms of the mesoionic ring in the higher occupied (HO) and lower unoccupied (LU) molecular orbitals.

$$\Delta E = \left[\frac{C_{2HO}\, C_{NLU} + C_{5HO}\, C_{CLU}}{E_{MHO} - E_{DLU}} + \frac{C_{2LU}\, C_{NHO} + C_{5LU}\, C_{CHO}}{E_{DHO} - E_{MLU}} \right] \beta^2 \qquad (2)$$

Analogously, C_{NHO}, C_{NLU}, C_{CHO}, and C_{CLU} are the corresponding coeficients on the N and C atoms of the dipolarophile in the HOMO and LUMO.

Terms (E_{MHO}- E_{DLU}) and (E_{DHO}- E_{MLU}) are the energy differences of the interacting pairs of occupied and unoccupied MOs of mesoionic heterocycle (M) and dipolarophile (D). The term β is the resonance integral that converts the efficiency of overlap into energy units.

The frontier orbital energy levels and their atomic orbital coeficients for **26** and **27** are represented in Table VIII.

Table VIII. Coeficients and Energy of HO and LU Molecular Orbitals from AM1 and MNDO Calculations

Comp		MO	Energy	C_1	C_2	C_3	C_4	C_5	C_N	C_C
26	MNDO	HO	-7.68	0.18	0.27	-0.11	-0.17	-0.65		
		LU	-1.18	0.37	-0.72	0.39	0.03	-0.28		
	AM1	HO	-7.32	-0.16	-0.20	0.03	0.21	0.60		
		LU	-0.88	-0.30	0.74	-0.39	-0.08	0.21		
27	MNDO	HO	-9.41						-0.23	-0.05
		LU	-0.24						-0.05	0.33
	AM1	HO	-9.25						0.33	0.22
		LU	-0.22						-0.10	0.40

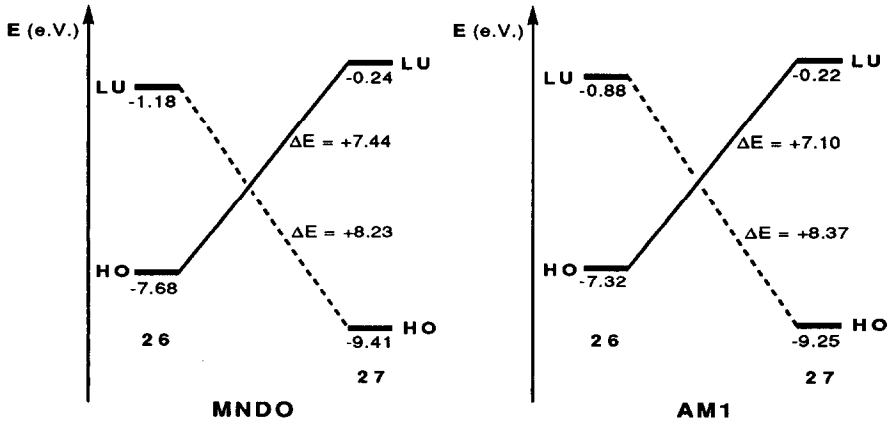

Figure 4. Energy diagram of FMOs for **26** and **27** from MNDO and AM1 calculations.

As shows the Figure 4, E_{MHO}- E_{DLU} is smaller than E_{DHO}- E_{MLU} for both calculation methods. For that, we can consider preponderant the HOMO (dipole)-LUMO (dipolarophile) interaction. However, the energy difference is too much short to neglect the second term of equation (2).

Similarly, for the regioisomer **29** the equation (3) must be considered:

$$\Delta E' = \left[\frac{C_{2HO}\, C_{CLU} + C_{5HO}\, C_{NLU}}{E_{MHO} - E_{DLU}} + \frac{C_{2LU}\, C_{CHO} + C_{5LU}\, C_{NHO}}{E_{DHO} - E_{MLU}} \right] \beta^2 \qquad (3)$$

The two interactions corresponding to both terms of eq. (2) and (3) are represented in the Figures 5 and 6, respectively, taking as reference the AM1 parameters.

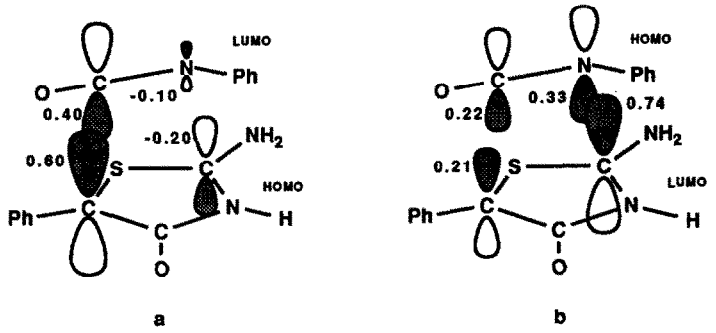

Figure 5

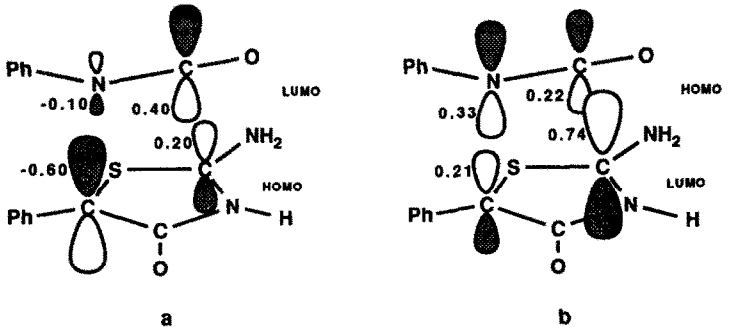

Figure 6

The FMO model[23] states that the (large x large) + (small x small) orbital coefficient interaction is better than the (large x small) + (small x large) one, which lead to the large sum of ΔE and dictates the orientation. Thus, the approach in parallel planes of **26** and **27** which furnishes the regioisomer **28** faces the higher coefficient sites in both HOMO (dipole) - LUMO (dipolarophile) (Figure 5a), and HOMO (dipolarophile) - LUMO (dipole) interactions (Figure 5b). The approach leading to the regioisomer **29** is otherwise less favoured (Figure 6).

Experimental

The ^{1}H- (200 MHz) and ^{13}C-NMR (50 MHz) spectra were recorded with a Bruker AC 200-E spectrometer. Assignments were confirmed by homo- and heteronuclear double-resonance experiments, and DEPT. Optical rotations were measured at 20±5º with a Perkin-Elmer 141 polarimeter. IR spectra (KBr discs) were recorded in the range 4000-600 cm^{-1} using a Perkin-Elmer 399 spectrophotometer and UV spectra (96% ethanol) with a Pye-Unicam SP8-250 instrument. EI mass spectra (35 and 70 eV) were obtained with a Kratos MS-80RFA mass spectrometer.

TLC was conducted on silica gel GF_{254} (Merck) with benzene-acetonitrile (3:1) and detection with UV light or iodine vapour. Melting points were determined on a Gallenkamp apparatus and are uncorrected. Microanalyses were carried out with a Perkin-Elmer 240C analyser.

Crystal data of 13

A systematic search in reciprocal space using a CAD4 Enraf-Nonius automatic diffractometer showed that crystals belong to the orthorhombic system.

The unit-cell dimensions and their standard deviations were obtained and refined at room temperature were with Mokα radiation (λ=0.7107) by using 25 carefully selected reflections. Final results: $C_{35}H_{33}N_3O_{10}$, mol.wt.=657.67, a=7.756(6), b=18.719(2), c=23.584(3)Å, V=3467Å^3, Z=4, d_{cal}=1.26 gcm^{-3}, μ=0.87 cm^{-1}, F(000)=1384, space group=$P2_12_12_1$.

A single crystal of 0.25x0.18x0.12 mm^3 was used and glued at the end of a glass wire mounted on a goniometer head. All quantitative data were obtained at room temperature on the same diffactometer using graphite monochromated radiation. The vertical and horizontal apertures in front of the counter were adjusted so as to minimize the background counts without loss of net peak intensity. The ω-2θ scan technique was used. 4071 reflections were recorded (2º<θ<28º). The resulting data was transferred to a VAX computer and for all subsequent calculations the X Ray System[25] was used.

Two standard reflections measured every hour during the complete data collection period showed only statistical fluctuations.

The collected data were converted into intensities and corrected for Lorentz and polarization factors. An unique data set of 988 reflections having I>2σ(I) was used to determine and refined the structure.

The structure was solved by direct methods using the MULTAN80 program[26]. After refinement of the heavy atoms, a difference-Fourier map revealed maxima of residuals electronic density close to the positions expected for the H atoms, they were introduced in the structure factor calculations, by their computed coordinates (C-H=1.00Å) and isotropic temperature factors as the atoms to which they are bonded, but not refined. Full-matrix least squares refinement was based on F (structure amplitudes) to minimize the function $\sum w(|F_o|-|F_c|)^2$ with $w=1/\sigma^2(F_o)$. The refinement led to a final convergence with R=0.09. All parameters shifts during the final cycle of refinement were <0.57; the residual electron density in the difference map revealed no significant maxima. Atomic scattering factors were taken from International Tables for X-Ray Crystallography[27].

Semiempirical calculations

Theoretical calculations were performed with the MNDO[20] and AM1[21] methods from the MOPAC programs system[28] on a CONVEX 210 computer. In all cases the geometries were calculated by minimizing the total energy with respect to *all* geometric variables. Special atention has been devoted to both methods in two exhaustive reviews[29] and a handbook[30] that have been recently published.

1-(4-Methoxyphenyl)-3,6-diphenyl-4-oxo-(3',5',6'-tri-*O*-acetyl-1',2'-dideoxy-α-D-gluco-furano)[1',2':4,5]-5a*H*,5b*H*-imidazo[1,2-*a*]pyrimidin-5-ylium-2-olate (13). To a stirred solution of **12** (3.0 g, 5.7 mmol) in dichloromethane (60 ml) was added 4-methoxyphenylisocyanate (0.75 ml, 5.7 mmol). The mixture was kept for 24 h at room temperature and concentrated to give an oily residue that crystallised from ethanol (0.9 g, 38%), mp 280-281ºC, $[\alpha]_D$ +40º, $[\alpha]_{578}$ +41.5º, $[\alpha]_{546}$ +49º, $[\alpha]_{436}$ +96º, (*c* 0.5, chloroform), λ_{max} 274 nm (ε_{mM} 42.3), m/z 655 (M$^+$), 553, 451, 331, 210, 149, 60, and 44. Anal. found: C, 63.89; H, 5.07; N, 6.33. Calcd. for $C_{35}H_{33}N_3O_{10}$: C, 64.12; H, 5.07; N, 6.41.

1-(4-Chlorophenyl)-3,6-diphenyl-4-oxo-(3',5',6'-tri-*O*-acetyl-1',2'-dideoxy-α-D-gluco-furano)[1',2':4,5]-5a*H*,5b*H*-imidazo[1,2-*a*]pyrimidin-5-ylium-2-olate (14). To a suspension of **12** (1.0 g, 1.9 mmol) in benzene (20 ml) was added 4-chlorophenylisocyanate (0.25 ml, 1.9 mmol). The

mixture was refluxed for 6 h, cooled to room temperature and chromatographed (benzene-acetonitrile 3:1) to give **14** (0.83 g, 65%), mp 171-173°C (ethanol-water), $[\alpha]_D$ +46°, $[\alpha]_{578}$ +48°, $[\alpha]_{546}$ +55°, $[\alpha]_{436}$ +100₀, (*c* 0.7, chloroform), λ_{max} 274 nm (ε_{mM} 12.6), m/z 659 (M^+), 557, 515, 406, 227, 153, 119, 90, 60, and 43. Anal. found: C, 61.72; H, 4.45; N, 6.09. Calcd. for $C_{34}H_{30}N_3O_9Cl$: C, 61.87; H, 4.58; N, 6.37.

1-(4-Nitrophenyl)-3,6-diphenyl-4-oxo-(3',5',6'-tri-*O*-acetyl-1',2'-dideoxy-α-D-gluco-furano)[1',2':4,5]-5a*H*,5b*H*-imidazo[1,2-*a*]pyrimidin-5-ylium-2-olate (15). A suspension of **12** (1.0 g, 1.9 mmol) in benzene (20 ml) was treated with 4-nitrophenylisocyanate (0.31 g, 1.9 mmol). The mixture was refluxed for 27 h and processed as described for **14** to give **15** (0.45 g, 36%), mp 186-187°C (ethanol-water), $[\alpha]_D$ +49°, $[\alpha]_{578}$ +53°, $[\alpha]_{546}$ +62°, (*c* 0.4, chloroform), λ_{max} 276 nm (ε_{mM} 17.9). Anal. found: C, 60.70; H, 4.52; N, 8.30. Calcd. for $C_{34}H_{30}N_4O_{11}$: C, 60.89; H, 4.51; N, 8.35.

1-(3-Methoxyphenyl)-3,6-diphenyl-4-oxo-(3',5',6'-tri-*O*-acetyl-1',2'-dideoxy-α-D-gluco-furano)[1',2':4,5]-5a*H*,5b*H*-imidazo[1,2-*a*]pyrimidin-5-ylium-2-olate (16). A suspension of **12** (3.0 g, 5.7 mmol) in benzene (60 ml) was treated with 3-methoxyphenylisocyanate (0.75 ml, 5.7 mmol). The mixture was refluxed for 22 h and cooled to room temperature to give **16** (2.49 g, 68%), mp 288-289°C (ethanol), $[\alpha]_D$ +22°, $[\alpha]_{578}$ +24°, $[\alpha]_{546}$ +28°, $[\alpha]_{436}$ +54°, (*c* 0.9, chloroform), λ_{max} 276 nm (ε_{mM} 9.0). Anal. found: C, 63.35; H, 5.06; N, 6.28. Calcd. for $C_{35}H_{33}N_3O_{10}$: C, 64.12; H, 5.07; N, 6.41.

1-(3-Chlorophenyl)-3,6-diphenyl-4-oxo-(3',5',6'-tri-*O*-acetyl-1',2'-dideoxy-α-D-gluco-furano)[1',2':4,5]-5a*H*,5b*H*-imidazo[1,2-*a*]pyrimidin-5-ylium-2-olate (17). The same procedure described above gave **17** (83%) from 3-chlorophenylisocyanate, mp 281-282°C (ethanol), $[\alpha]_D$ +16.5°, $[\alpha]_{578}$ +18°, $[\alpha]_{546}$ +20°, $[\alpha]_{436}$ +36°, (*c* 1.0, chloroform), λ_{max} 274 nm (ε_{mM} 14.3). Anal. found: C, 62.03; H, 4.70; N, 6.31. Calcd. for $C_{34}H_{30}N_3O_9Cl$: C, 61.87; H, 4.58; N, 6.37.

1-(3-Nitrophenyl)-3,6-diphenyl-4-oxo-(3',5',6'-tri-*O*-acetyl-1',2'-dideoxy-α-D-gluco-furano)[1',2':4,5]-5a*H*,5b*H*-imidazo[1,2-*a*]pyrimidin-5-ylium-2-olate (18). Compound **12** (1.0 g, 1.9 mmol) with 3-nitrophenylisocyanate (0.24 ml, 1.9 mmol) as described for **16.** The solvent was evaporated to give an oily residue which crystallised from ethanol (0.81 g, 65%), mp 262-263°C, $[\alpha]_D$ +1°, $[\alpha]_{578}$ +1°, $[\alpha]_{546}$ -0.5°, $[\alpha]_{436}$ -28°, (*c* 0.8, chloroform), λ_{max} 274 nm (ε_{mM} 23.8). Anal. found: C, 60.86; H, 4.53; N, 8.40. Calcd. for $C_{34}H_{30}N_4O_{11}$: C, 60.89; H, 4.51; N, 8.35.

1-(2-Methoxyphenyl)-3,6-diphenyl-4-oxo-(3',5',6'-tri-*O*-acetyl-1',2'-dideoxy-α-D-gluco-furano)[1',2':4,5]-5a*H*,5b*H*-imidazo[1,2-*a*]pyrimidin--5-ylium-2-olate (19). A suspension of **12** (1.0 g, 1.9 mmol) in benzene (20 ml) was treated with 2-methoxyphenylisocyanate (0.23 ml, 1.9 mmol). The mixture was refluxed for 42 h and cooled to room temperature to give **19** (0.34 g, 28%), mp 296-297°C, $[\alpha]_D$ -46°, $[\alpha]_{578}$ -40°, $[\alpha]_{546}$ -47°, $[\alpha]_{436}$ -90°, (*c* 0.7, chloroform), λ_{max} 277 nm (ε_{mM} 16.8), m/z 655 (M^+), 553, 525, 210, 60, and 44. Anal. found: C, 64.08; H, 5.19; N, 656. Calcd. for $C_{35}H_{33}N_3O_{10}$: C, 64.12; H, 5.07; N, 6.41.

1-(2-Chlorophenyl)-3,6-diphenyl-4-oxo-(3',5',6'-tri-*O*-acetyl-1',2'-dideoxy-α-D-gluco-furano)[1',2':4,5]-5a*H*,5b*H*-imidazo[1,2-*a*]pyrimidin-5-ylium-2-olate (20). Following the same procedure described for **19**, compound **20** (46%) was obtained from 2-chlorophenylisocyanate after 3 h of reflux, mp 225-226°C (ethanol), $[\alpha]_D$ +26°, $[\alpha]_{578}$ +28°, $[\alpha]_{546}$ +32°, $[\alpha]_{436}$ +60°, (*c* 0.8, chloroform), λ_{max} 274 nm (ε_{mM} 15.4), m/z 670 (M^+), 406, 222, 194, 60, and 43. Anal. found: C, 62.02; H, 4.70; N, 6.30. Calcd. for $C_{34}H_{30}N_3O_9Cl$: C, 61.87; H, 4.58; N, 6.37.

1-(2-Nitrophenyl)-3,6-diphenyl-4-oxo-(3',5',6'-tri-*O*-acetyl-1',2'-dideoxy-α-D-gluco-furano)[1',2':4,5]-5a*H*,5b*H*-imidazo[1,2-*a*]pyrimidin-5-ylium-2-olate (21). Following the same procedure described for **19**, compound **21** (64%) was obtained from 2-nitrophenylisocyanate after 6 h of reflux, mp 260-261°C (ethanol), $[\alpha]_D$ -51°, $[\alpha]_{578}$ -52°, $[\alpha]_{546}$ -66.5°, (*c* 0.9, chloroform), λ_{max} 273 nm (ε_{mM} 19.4). Anal. found: C, 60.61; H, 4.62; N, 8.13. Calcd. for $C_{34}H_{30}N_4O_{11}$: C, 60.89; H, 4.51; N, 8.35.

Acknowledgements. This work was supported by DGICYT (PB89-0492 and PB89-0540). We are also grateful to Dr. P. Cintas for his helpful discussions.

References

1 Potts, K. T. Mesoionic Ring Systems. In *1,3-Dipolar Cycloaddition Chemistry;* Padwa, A.; Ed.; John Wiley and Sons, Inc.: New York, 1974, Vol. 2, pp.1-82.
2 Ollis, W. D.; Stanforth, S. P.; Ramsden, C.A.*Tetrahedron* **1985**, *41*, 2239-2329.
3 Potts, K. T.; Husain, S. *J. Org. Chem.* **1972**, *37*, 2049-2050.
4 Potts, K. T.; Baum, J.; Houghton, E.; Roy, D. N.; Singh, U. P. *J. Org. Chem.* **1974**, *39*, 3619-3627.
5 Potts, K. T.; Baum, J.; Datta, S. K.; Houghton, E. *J. Org. Chem.* **1976**, *41*, 813-818.
6 Hamaguchi, M.; Nagai, T. *J. Chem. Soc., Chem. Commun.* **1985**, 726-728.
7 Potts, K. T.; Huang, F.; Khattak, R. K. *J. Org. Chem.* **1977**, *42*, 1644-1648.
8 Previously, a similar transformation was performed from a 1,3,4-thiadiazolium-5-thiolate system and dimethyl azodicarboxylate: Moriarty, R. M.; Kliegmann, J. M.; Besai, R. B. *Chem. Commun.* **1967**, 1045-1046.
9 Areces, P.; Avalos, M.; Babiano, R.; González, L.; Jiménez, J. L.; Palacios, J. C.; Pilo, M. D. *Carbohydr. Res.* **1991**, *222*, 99-112.
10 Kappe, T. *Wiss. Z. Karl-Marx-Univ. Leipzig, Math.-Naturwiss. R.* **1983**, 32, 437-446.
11 Kappe, T. *Lect. Heterocycl. Chem.* **1984**, *7*, 107-119.
12 Cremer, D.; Pople, J. A. *J. Am. Chem. Soc.* **1975**, *97*, 1354-1358.
13 Nardelli, M. *Acta Crystallogr.* **1983**, *C39*, 1141-1142.
14 Avalos, M.; Jiménez, J. L., Palacios, J. C.; Ramos, M. D.; Galbis, J. A. *Carbohydr. Res.* **1987**, *167*, 49-64.
15 Avalos, M.; Cintas, P.; Gómez, I. M.; Jiménez, J. L.; Palacios, J. C.; Rebolledo, F.; Fuentes, J. *Carbohydr. Res.* **1989**, *187*, 1-14.
16 Sandström, J. *Dynamic NMR Spectroscopy;* Academic Press: London. 1982; pp. 77-91.
17 Lönngren, J.; Svensson, S. *Adv. Carbohydr. Chem. Biochem.* **1974**, *29*, 41-106.
18 Areces, P.; Avalos, M.; Babiano, R.; González, L.; Jiménez, J. L.; Méndez, M. M.; Palacios, J. C. unpublished results.
19 Baudy, M.; Robert, A.; Guimon, C. *Tetrahedron* **1982**, *38*, 1241-1252 ; *ibid.* 2129-2137.
20 Dewar, M. J. S.; Thiel, W. *J. Am. Chem. Soc.* **1977**, *99*, 4899-4907; *ibid.* 4907-4917.
21 Dewar, M. J. S.; Zoebisch, E. G.; Healy, E. F.; Stewart, J. J. P. *J. Am. Chem. Soc.* **1985**, *107*, 3902-3909.
22 Pimentel, G. C.; McClellan, A. L. *The Hydrogen Bond*; W. H. Freeman: New York. 1960.
23 Huisgen, R. 1,3-Dipolar Cycloadditions. Introduction, Survey, Mechanism. In *1,3-Dipolar Cycloaddition Chemistry* Padwa, A. Ed.; John Wiley and Sons, Inc.: New York, 1984; Vol. 1, pp. 1-176.
24 Fukui, K. *Acc. Chem. Res.* **1971**, *4*, 57-64.
25 Stewart, J. M.; Kundell, F. A.; Baldwin, J. C. *The X-Ray System*; Computer Science Center, University of Maryland, College Park. 1970.
26 Main, P.; Fiske, S. J.; Hull, S. E.; Lessinger, L.; Germain, G.; Declercq, J. P.; Woolfson, M. M *Multan80, A System of Computer Programs for the Automatic Solution of Crystal Structures from X-Ray Diffraction Data;* Universities of York (England) and Louvain (Belgium). 1980.
27 *International Tables for X-Ray Crystallography;* Kynoch Press: Birmingham. 1962; Vol. III.
28 Stewart, J. J. P. *MOPAC*, QCPE n455. 1983.
29 a)Thiel, W. *Tetrahedron*, **1988**, *44*, 7393-7408; b) Stewart, J. J. P. *Reviews in Computational Chemistry;* VCH Publishers: New York. 1990; p. 45.
30 Clark, T. *A Handbook of Computational Chemistry;* John Wiley and Sons: New York. 1985.